Applied Catalysis A: General 402 (2011) 121–131

Contents lists available at ScienceDirect

Applied Catalysis A: General

journal homepage: www.elsevier.com/locate/apcata

The role of alkali modifiers (Li, Na, K, Cs) in activity of 2%Pd/Al_2O_3 catalysts for 2-ethyl-9,10-anthraquione hydrogenation

R. Kosydar, A. Drelinkiewicz*, E. Lalik, J. Gurgul

Institute of Catalysis and Surface Chemistry, Polish Academy of Sciences, 30-238 Kraków, Niezapominajek 8, Poland

ARTICLE INFO

Article history:
Received 22 February 2011
Received in revised form 25 May 2011
Accepted 26 May 2011
Available online 2 June 2011

Keywords:
2-Ethylanthraquinone
Palladium catalysts
Hydrogenation
Alkali modifier

ABSTRACT

Present research concentrates on the role of alkali modifiers (Li, Na, K, Cs) in activity of 2%Pd/Al_2O_3 catalyst for 2-ethyl-9,10-anthraquinone (eAQ) hydrogenation. The catalysts with various content of alkali modifier (Me/Pd molar ratio ranges from 0.5 up to 4, Me-alkali metal) were prepared by impregnation of pre-reduced 2%Pd/Al_2O_3 catalyst with appropriate alkali metal carbonates. The XPS, EDS and TEM measurements show that alkali promoters are introduced into alumina matrix. The microcalorimertic experiments of CO adsorption prove the interaction of CO with catalysts leading to stronger bonding of carbon monoxide by alkali doped catalysts. The presence of alkali promoters in Pd/Al_2O_3 catalyst plays an essential role in the whole eAQ hydrogenation process. The nature of alkali promoter and its content (Me/Pd atomic ratio) in catalyst are of importance. As the alkalinity of promoter increases going from Li to Cs all the effects caused by their presence become stronger. In the presence of alkali doped catalysts the content of 2-ethyloxoanthrone (OXO, isomer of 2-ethyl-9,10-anthrahydroquinone) formed is higher than that on un-doped 2%Pd/Al_2O_3. On the other hand, reactions in the "deep hydrogenation" stage comprising the formation of 2-ethyl-5,6,7,8-tetrahydro-9,10-anthraquinone (H_4eAQ) and the transformation of OXO to 2-ethylanthrone and other degradation products are remarkably inhibited. In particular, the formation of 2-ethylanthrone via hydrogenolysis of OXO isomer is strongly suppressed. The Cs-doped catalyst exhibits the highest activity to OXO among all the catalysts tested whereas the ability of Cs-doped catalysts to the formation of anthrone is most effectively inhibited. The role of alkali modifiers is considered to be associated with stronger interactions between the catalyst and quinone reagents, and in particular OXO isomer. Moreover, in the reagent adsorption the centres of support nearby the palladium particles may also participate by affecting the mode of reagents adsorption.

1. Introduction

The catalytic hydrogenation of 2-ethyl-9,10-anthraquinone (eAQ) into 2-ethyl-9,10-anthrahydroquinone ($eAQH_2$) is one of the key steps in the industrial synthesis of hydrogen peroxide [1,2]. In this method eAQ is hydrogenated in the presence of supported palladium catalysts to yield 2-ethyl-9,10-anthrahydroquinone ($eAQH_2$). Oxidation of $eAQH_2$ results in hydrogen peroxide with the regeneration of starting eAQ. However, even on the most selective catalyst, eAQ slowly disappears due to its consumption in various side reactions yielding number of products termed as "degradation products". They are not oxidized to form H_2O_2 and thus represent a loss of starting eAQ [3–7]. Reduction of the content of degradation products formed in the conventional route of hydrogen peroxide synthesis is an important aspect of process improvement, since the formation of these by-products substantially reduces the amount of active quinones, eAQ and 2-ethyl-5,6,7,8-tetrahydro-9,10-anthraquinone (H_4eAQ) [6]. It has been demonstrated by Chen [6] that in industrial practice the selectivity of the desired reaction, i.e. hydrogenation of quinone to hydroquinone should be above 99%. However, in cyclic hydrogenation/oxidation operations, the degradation products accumulate in the solution and consequently a regeneration step has to be involved. This clearly shows that the contribution of side reactions consuming active quinones must be strongly limited. Thus, better understanding the course of side reactions yielding degradation products become one of the priority issues in developing industrial anthraquinone process [6].

The degradation products are formed in reactions involving carbonyl group, such as the hydrogenolytic cleavage of C–O bonds producing mainly 2-ethylanthrone (eAN). Upon further hydrogenation, eAN is slowly converted to products containing hydrogenated

Abbreviations: eAQ, 2-ethyl-9,10-anthraquinone; $eAQH_2$, 2-ethyl-9,10-anthrahydroquinone; OXO, 2-ethyl-10-hydroxy-9-anthrone (2-ethyloxanthrone); H_4eAQ, 2-ethyl-5,6,7,8-tetrahydro-9,10-anthraquinone; H_4eAQH_2, 2-ethyl-5,6,7,8-tetrahydro-9,10-anthrahydroquinone; H_8eAQ, 2-ethyl-1,2,3,4,5,6,7,8-octahydro-9,10-anthraquinone; eAN, 2-ethylanthrone (2-ethyl-10-anthrone and 2-ethyl-9-anthrone); H_4eAN, 2-ethyl-5,6,7,8-tetrahydroanthrone.

* Corresponding author.
E-mail address: drelinki@chemia.uj.edu.pl (A. Drelinkiewicz).

0926-860X/$ – see front matter © 2011 Published by Elsevier B.V.
doi:10.1016/j.apcata.2011.05.036

Table 1
Physicochemical characteristic of catalysts.

Catalyst	BET surface area (m^2/g)	Porosity (cm^3/g)	Pore size (nm)	Surface concentration (at%) obtained by EDS, average data							
				As-prepared catalysts				Recovered catalysts			
				Al	Pd	Me	Me/Pd	Al	Pd	Me	Me/Pd
Pd/Al	165	0.27	4.3	97.4	2.6						
Li–Pd/Al	162	0.27	4.3								
0.5Na–Pd/Al				95.6	3.3	1.1	0.33	97.1	2.3	0.9	0.39
Na–Pd/Al	149	0.25	4.3	95.3	2.5	1.85	0.74	95.2	2.7	2.1	0.77
K–Pd/Al				95.5	2.7	1.80	0.67	96.2	2.3	1.5	0.65
Cs–Pd/Al	154	0.25	3.8	95.6	2.6	1.80	0.69	96	2.1	1.8	0.85
4Cs–Pd/Al	158	0.20	3.8	88.5	2.3	9.2	4	88.6	2.4	9	3.8

aromatic ring (2-ethyl-5,6,7,8-tetrahydroanthrone H_4eAN) as well as to 2-ethylanthracene (eANT) [8–10]. However, apart from the degradation reactions, a successive saturation of phenyl ring in $eAQH_2$ to give H_4eAQ (active quinone) and 2-ethyl-1,2,3,4,5,6,7,8-octahydro-9,10-anthraquinone (H_8eAQ) takes place. The literature data showed that the hydrogenolytic C–O reactions are preceded by the tautomerization of hydroquinone form to 2-ethyl-10-hydroxy-9-anthrone (2-ethyloxoanthrone) (OXO) (Scheme 1) [1,2,11–13]. In case of anthraquinone molecule, the equilibrium concentrations of enol–keto forms in solutions were reported to depend on medium properties and, accordingly, acidic conditions favoured the formation of keto-form [12,13]. Hence, during the consumption of a desired hydroquinone-form a number of consecutive and parallel reactions can be observed which are known as "deep hydrogenation" stage. In our continuing work concentrating on variables determining the course of quinone degradation we focused our attention on studying the role of alkaline promoters Li, Na, K and Cs in catalytic performance of Pd/Al_2O_3. The present studies have been undertaken because our previous results showed that highly alkaline medium formed due to high content of Na_2CO_3 in Pd/SiO_2 catalyst together with humidity in the eAQ solution enhanced the transformation of eAQ via hydrogenolytic reactions which produced degradation products [14]. On the other hand, a beneficial effect of modifiers as alkali and alkali earth metals on the behaviour of Pd-catalysts in terms of catalytic activity, selectivity and resistance to deactivation was observed in various reactions, among them hydrogenation of α, β-unsaturated aldehydes (cinnamyl and crotyl) [15–17], aromatic ketones (acetophenone) [18], phenols [19–22] as well as alkynes such as 2-butyne-1,4-diol [23]. An electronic effect, induced by alkali over the metal particles has been stressed by several authors to explain these activity and selectivity changes [15]. Accordingly, the alkali promoter tends to donate electron to the metal which leads to higher charge density of the palladium particles. The promoting roles of sodium in Pd/C catalyst observed in hydrogenation of biphenol [22] as well as strontium in supported Pd-catalysts (Al_2O_3, SiO_2, MgO, hydrotalcite, zeolite) during hydrogenation of phenol [20] were explained by electronic effects. The increase in basicity of $Pt/CaCO_3$ catalysts due to doping with Li, Na, K and Cs-carbonates was reported to be responsible for the increase in electron density of Pt which resulted in more selective hydrogenation of C≡C in 2-butyne-1,4-diol to form olefinic diol, 2-butene-1,4-diol [23]. An enhanced activity and selectivity of alkali (Li, Na, K) doped Pt/graphite for hydrogenation of α, β-unsaturated aldehydes to alcohols was related to the presence of electropositive metal which after donation of electrons to platinum becomes a highly active centre for the activation of C=O group thus facilitating its adsorption [15–17]. Cinnamaldehyde was adsorbed on the modifier surface via donation of a lone pair of electrons from the oxygen atom [17].

The role of alkali promoters (Ca, K, Cs) in hydrogenation of phenol to cyclohexanone on Pd/Al_2O_3 catalyst was explained by the modification of acid–base properties of alumina support due to partial neutralization of acid sites and generation of basic sites [19,21]. The authors concluded that phenol was adsorbed on the surface of the support through the oxygen of the O–H group as a phenolate species and high basicity of the support stabilized the phenolate forms. Reaction occurred mainly between such phenolate species and hydrogen activated on the Pd-sites [19,21].

In the present work $2\%Pd/Al_2O_3$ catalysts modified by alkali Li, Na, K and Cs-promoters were prepared by impregnation technique. The effect of the nature of alkali promoter as well as its content in catalysts was studied. Particular attention was focused on the role of alkali promoters in the hydrogenation of quinone reduced forms, namely $eAQH_2$ and its tautomer OXO.

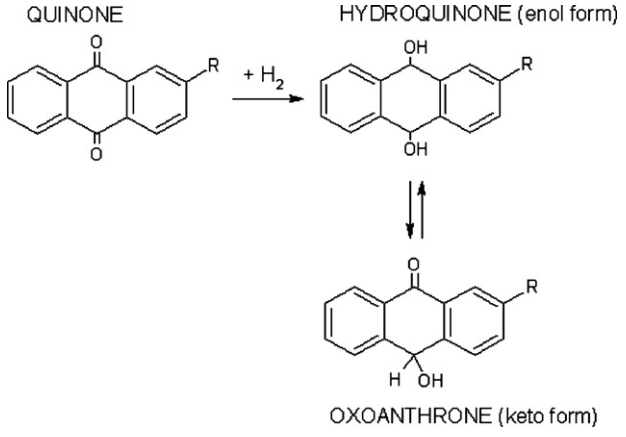

Scheme 1. Tautomerization equilibrium of hydroquinone–oxoanthrone forms.

2. Experimental

2.1. Preparation of catalysts

$2\%Pd/Al_2O_3$ catalyst (abbreviated as Pd/Al) was prepared using alumina support γ-Al_2O_3, Procatalyse, SPH 1515 batch, grain diameter 50–150 μm, the content of Na as Na_2O was given by Manufacturer to be 670 ppm. The support was impregnated with $PdCl_2$ solution of very low acidity (pH ~4) prepared using 0.06 M HCl ($PdCl_2$ concentration 2.3×10^{-3} mol/dm^3). The obtained sample was calcined in air at 450 °C for 5 h and reduced with hydrogen at 300 °C for 3 h. The catalyst was stored in a desiccator until use. It should be stressed that prior to the catalytic experiments, the catalysts were activated with hydrogen "in situ" in the reactor.

Alkali doped catalysts were prepared by impregnation of the pre-reduced $2\%Pd/Al_2O_3$ catalyst with an aqueous solution of appropriate alkali metal carbonates (concentration 2.83×10^{-2} mol/dm^3), namely Li_2CO_3, Na_2CO_3, K_2CO_3 and Cs_2CO_3. The sample of $2\%Pd/Al_2O_3$ catalyst (dried overnight at 120 °C) was

added into solution of alkali metal carbonates and impregnation was carried out at temperature of 80–90 °C up to complete evaporation of liquid. The obtained alkali doped catalysts were dried overnight at 120 °C. In typical procedure the catalysts of Me/Pd molar ratios of ca. 0.7 were obtained (Table 1). By changing the volume of alkali carbonate solutions, the catalysts having their respective ratios of Na/Pd and Cs/Pd other than 0.7 were also prepared. The alkali doped catalysts of typical Me/Pd molar ratio of ca. 0.7 are abbreviated as Li–Pd/Al, Na–Pd/Al, K–Pd/Al and Cs–Pd/Al. For catalysts having a different content of alkali promoter the ratio of Me/Pd is given before the name (4Cs–Pd/Al corresponds to Cs/Pd ~ 4).

2.2. Characterization of catalysts

The specific surface areas of samples were calculated from the nitrogen adsorption–desorption isotherms at 77 K in an Autosorb-1, Quantachrome equipment. Prior to the measurements, the samples were heated at 120 °C for 16 h.

The X-ray photoelectron spectroscopy (XPS) measurements were carried out with a hemispherical analyzer (SES R4000, Gammadata Scienta). The unmonochromatized Al Kα (1486.6 eV) X-ray source with the anode operating at 11 kV and 17 mA current emission was applied to generate core excitation. All binding energy values were charge-corrected to the carbon C 1s excitation which was set at 285.0 eV. The samples were pressed into indium foil and mounted on a special holder. All spectra were collected at pass energy of 100 eV except survey scans which were collected at pass energy of 200 eV. Intensities were estimated by calculating the integral of each peak, after subtraction of the Shirley-type background, and fitting the experimental curve with a combination of Gaussian and Lorentzian curves of variable proportions (70:30).

Field emission scanning electron microscope JEOL JSM – 7500 F equipped with the X-ray energy dispersive (EDS) system was used for the X-ray (EDS) measurements of surface concentration (at%) of Al, Pd and alkali promoters Na, K, Cs in catalysts.

TEM and STEM studies were performed on FEI Tecnai G^2 transmission electron microscope operating at 200 kV equipped with EDAX EDX and HAADF/STEM detectors. Samples for analysis were prepared by placing a drop of the suspension of sample in ethanol or THF onto a carbon-coated copper grid, followed by evaporating the solvent.

2.3. Microcalorimetry of CO adsorption

The experiments were performed using the Microscale gas flow-through microcalorimeter. A mixture of 3% CO in diluent nitrogen was used for all experiments. The amount of catalyst (ca. 0.16 g, of catalyst, corresponds to ca. 30 μmol of Pd) was such to fill the microcalorimetric cell of ca. 0.15 cm^3. The flow-through measurements of CO adsorption were carried out at RT and atmospheric pressure, with the flow rate of gas mixture 3 cm^3/min. The catalyst was first heated at 105 °C (16 h) in the flow of nitrogen and then subjected to an adsorption/desorption cycle of hydrogen at the same temperature in order to remove the surface oxygen. Following this pre-treatment, the sample was cooled down in the flow of nitrogen and the system was equilibrated thermally at RT. The adsorption measurement was initiated by replacing the nitrogen gas by the mixture of N_2 with 3% CO. The calorimetric curve was recorded and concurrently the uptake of CO was measured using a down-stream thermoconductivity detector (TCD). Calibration was made "in situ" for each measurement using a Teflon-encapsulated electric coil located axially and surrounded by the sample within the microcalorimetric cell.

2.4. Hydrogenation experiments

Hydrogenation of eAQ was performed in agitated glass reactor at atmospheric pressure of hydrogen and temperature of 55 °C following a previously described procedure [9,14]. A mixture of p-xylene and 2,6-dimethylheptane-4-ol (diisobutyl carbinol) with the volume ratio of 8:2 was used as the solvent system. Before the hydrogenation experiment the catalyst was wetted with reagent solution and was activated "in situ" inside the reactor by passing through the reactor at first nitrogen gas (15 min) and then hydrogen gas (20 min at room temperature and then for next 15 min at 55 °C). Following this procedure, the reaction was started by contacting the catalyst with the hydrogenated solution. The progress of hydrogenation was followed by measuring hydrogen uptake as a function of reaction time. In a typical hydrogenation experiment 0.45 g of catalyst in 30 cm^3 of solution (initial eAQ concentration 20 g/dm^3) was used and the reaction was carried out up to reaching a consumption of ca. 2–3 mol of H_2 per 1 mol of anthraquinone initially present in the reactor. Reproducibility of the hydrogenation experiments was ca. 5% over 2–3 catalysts batches.

In the course of reaction the samples of solution were taken at appropriate time intervals and the composition of solution was analysed by HPLC following the analytical methods described in our previous papers [9,14]. The concentration of reagents eAQ, H_4eAQ, eAN (2-ethylanthrone) and OXO at reaction time t (number of moles at time t: $\{n^t(\text{eAQ})\}$, $\{n^t(\text{H}_4\text{eAQ})\}$, $\{n^t(\text{eAN})\}$ and $\{n^t(\text{OXO})\}$) was analysed by HPLC in a re-oxidized solution.

The conversion of eAQ (K, %), selectivity to H_4eAQ (S-Tetra, %) and selectivity to anthrone (S-eAN, %) were calculated according to the equations

$$K = \frac{n^t(\text{eAQ})}{n^o(\text{eAQ}) - n^t(\text{eAQ})} \times 100\% \quad (1)$$

where n^o(eAQ), initial concentration of eAQ

$$\text{S-Tetra} = \frac{n^t(\text{H}_4\text{eAQ})}{n^o(\text{eAQ}) - n^t(\text{eAQ})} \times 100\% \quad (2)$$

$$\text{S-eAN} = \frac{n^t(\text{eAN})}{n^o(\text{eAQ}) - n^t(\text{eAQ})} \times 100\% \quad (3)$$

Compounds termed "degradation products" were analysed also by GC–MS method [9]. Reproducibility of the chromatographic analysis was ca. 5%.

3. Results and discussion

The textural properties of studied catalysts are collected in Table 1. The specific surface area and porosity of initial un-doped 2%Pd/Al_2O_3 catalyst only slightly decrease after modification by alkali promoters. Likewise, the average pore diameter only slightly decreases from 4.3 nm in the un-doped Pd/Al to 3.8 nm in the Cs–Pd/Al catalyst. It indicates that the original pore structure of 2%Pd/Al_2O_3 catalyst remains largely unaffected by doping with typical amount of alkaline promoters (Me/Pd ~ 0.7). The X-ray energy dispersive measurements (EDS) showed the presence of Al, Pd and alkaline promoters whereas no Cl was observed. The surface concentrations (average data, in at%) of Al, Pd and alkaline promoters, Na, K, Cs determined by EDS are collected in Table 1. The measurements were performed for fresh catalysts and for selected samples removed from the reactor after the hydrogenation experiment. No sodium was detected by the EDS in the un-doped Pd/Al catalyst, which is in agreement with the composition of alumina support given by the manufacturer (see Section 2). The lithium content could not be determined by the EDS technique in the Li–Pd/Al catalyst because of too low sensitivity of the method for this element. The Me/Pd atomic ratios of "typical" catalysts, namely Na–Pd/Al,

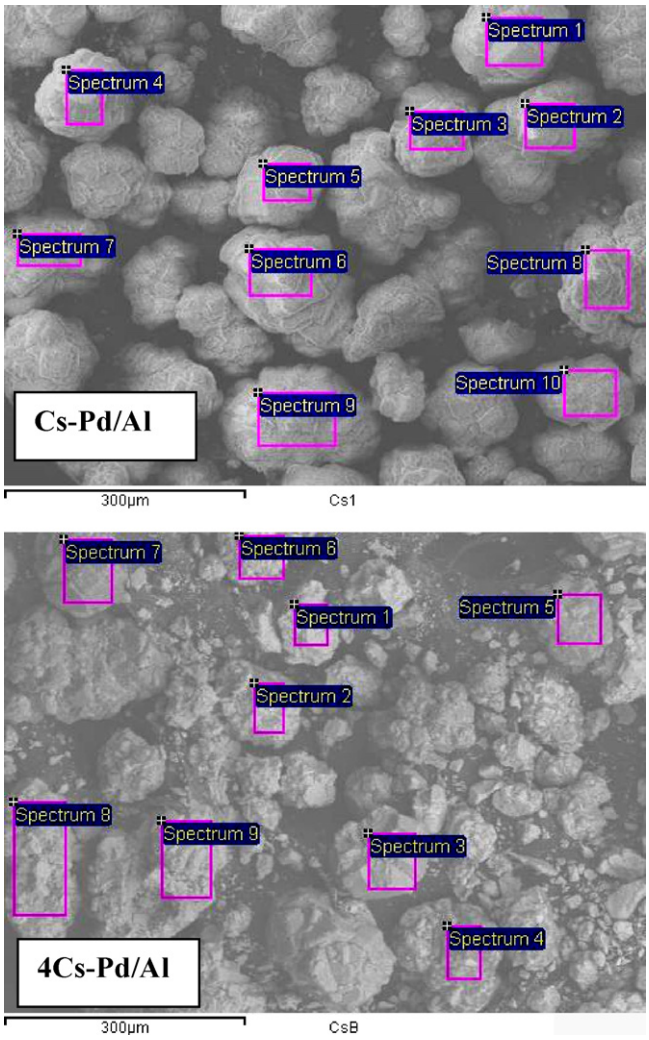

Fig. 1. SEM micrographs of Cs–Pd/Al and 4Cs–Pd/Al catalysts with marked areas where EDS analysis was performed.

K–Pd/Al and Cs–Pd/Al are practically the same, within the range 0.67–0.74. At this loading of alkaline promoter, its distribution throughout the catalyst grains was practically homogenous in all studied catalysts. As an example the data obtained for Cs–Pd/Al catalyst are provided showing almost constant surface concentration of Cs in all areas analysed by the EDS technique (Fig. 1 and Table 2). Doping of initial Pd/Al catalyst with a content of Cs_2CO_3 3-times higher than that in "typical" procedure resulted in certain non-homogeneity of Cs distribution evidenced by visible differences in

Table 2
Surface concentration of Al, Cs and Pd (in at%) determined by EDS technique for Cs–Pd/Al and 4Cs–Pd/Al catalysts.

Spectrum	Cs–Pd/Al				4Cs–Pd/Al			
	Al	Cs	Pd	Cs/Pd	Al	Cs	Pd	Cs/Pd
1	95.9	1.4	2.7	0.52	83.7	15.7	0.6	26.2
2	95.7	1.5	2.8	0.54	86.5	12.1	1.3	9.30
3	97.3	1.4	1.3	1.1	92.6	6.3	1.2	5.25
4	96.2	1.6	2.1	0.76	91.0	7.2	1.9	3.79
5	96.1	1.8	2.1	0.86	93.1	5.1	1.8	2.83
6	96.5	1.5	2.0	0.75	85.5	14.1	0.4	35.2
7	95.9	1.9	2.2	0.86	92.9	4.4	2.7	1.63
8	96.5	1.7	1.8	0.94	91.0	8.5	0.5	17.0
9	95.9	2.0	2.1	0.95	89.7	9.5	0.8	11.9
10	96.3	1.6	2.1	0.76				

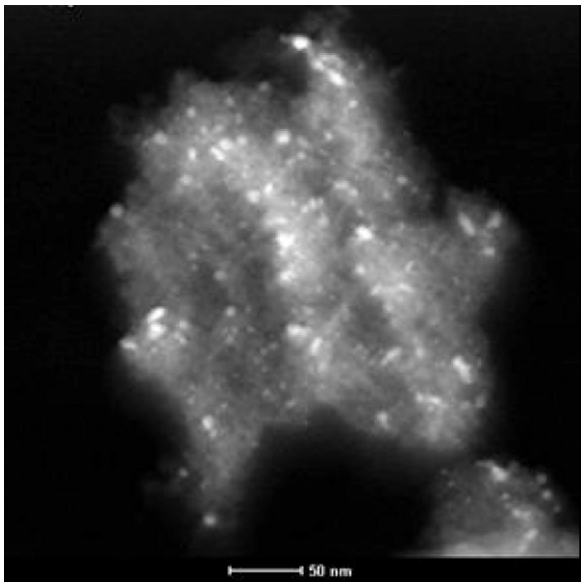

Fig. 2. STEM micrograph of un-doped 2%Pd/Al_2O_3 catalyst.

the surface concentrations of Cs at different areas on the catalyst surface. This effect was even stronger at 4-times higher loading of Cs (catalyst 4Cs–Pd/Al), in which case a few analysed areas showed the concentration of Cs markedly higher than a majority of other analysed places (Fig. 1 and Table 2). Thus, at the high loading of Cs (Cs/Pd ~ 3–4), an accumulation of some of Cs-species occurs and, as a result, a number of areas enriched with cesium appear on the catalyst surface.

The EDS data for the recovered catalysts (Table 1) show that the composition of catalysts in general and in particular the Me/Pd atomic ratio is preserved after the hydrogenation experiments. This was observed within the whole range of Me/Pd ratios in the catalysts.

The micrographs of the un-doped Pd/Al and the cesium doped 4Cs–Pd/Al catalysts obtained by the HAADF STEM registration mode of transmission electron microscope are displayed in Figs. 2 and 3, respectively. This registration mode is sensitive to Z-number of elements and provides the micrographs in which the Pd particles are bright spots whereas the support is black field. Moreover, electron diffraction as well as EDS analyses can be performed using this registration mode.

In the micrographs of both catalysts a number of Pd-particles of size within wide range, 2–10 nm is observed. The individual Pd-particles as well as their aggregates appear in both catalysts and no essential difference in the Pd-particles state can be observed. In order to better recognize the location of alkali promoter the EDS analysis was performed along the line marked in Fig. 3. It can be observed that the bright spots represent the areas enriched with Pd (Pd particles) whereas cesium is distributed throughout the whole catalyst. It indicates that similarly to what was observed for alumina supported catalysts [19,21], cesium appears to be introduced into the alumina support. This conclusion is also supported by the results of XPS studies (Figs. 4–6). The XPS spectra of Pd 3d, Al 2p and C 1s were registered for un-doped Pd/Al and two alkali doped Li–Pd/Al and Cs–Pd/Al catalysts. In the spectrum of un-doped Pd/Al catalyst only one state of Al at binding energy of 74.5 eV appears which is in agreement with the energy of 74.7 eV reported in the literature for Pd/γ-Al_2O_3 sample [24]. On the other hand, the spectra of Li and Cs-doped catalysts both show two states of Al-species. Apart from the Al 2p energy of 74.5 eV, a small contribution of new Al state of higher binding energy can be observed (Fig. 4). It should be stressed that binding energy may change depending on the near-

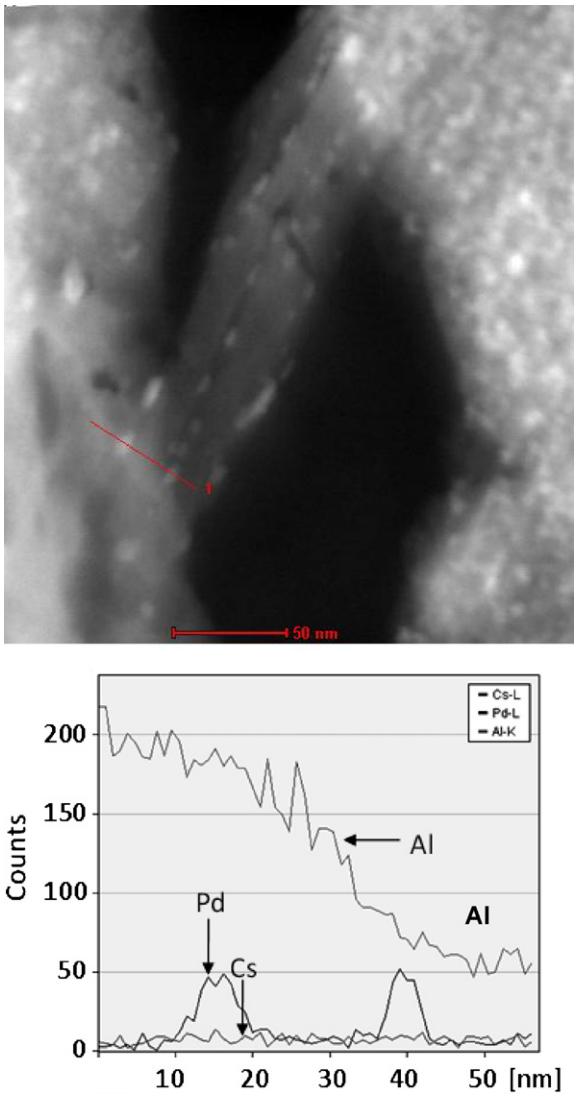

Fig. 3. STEM micrograph of cesium doped 4Cs–Pd/Al catalyst and the distribution of Pd and Cs along the marked line determined by EDS analysis.

est environment of the atom because this energy is determined by the electron density. In fact, higher values of Al 2p binding energy were reported for number of compounds, for example $MgAl_2O_4$ 76.3 eV, $Al(OH)_3$ 75.7–75.9 eV, AlO(OH) 76.7 eV [24]. Thus, the formation of a new Al state in the present catalysts can be explained as a result of interaction between lithium or cesium-species and alumina support. This observation is consistent with the results reported by Qi et al. [25] who showed that the addition of alkali modifier affected the acid–base properties of the alumina support. This was result of strong interaction between the modifier and the vacant site of alumina support [25].

In the XPS C 1s spectra of all three un-doped and alkali-doped catalysts a strong peak at binding energy of 285 eV dominates. This carbon energy is commonly detected in samples subjected to the XPS technique and is ascribed to the presence of carbon contaminations. However, in the spectra of alkali-doped catalysts (Fig. 5) a new carbon state at energy of 289.2 eV is observed. This energy is commonly ascribed to the carbon in carbonate CO_3^{2-} ions [24]. This shows incorporation of lithium/cesium carbonates into alumina support. However, the presence of other Li, Cs-species, like hydroxide cannot be excluded because of using aqueous solutions of alkali carbonates. On the other hand, no remarkable changes in the Pd state are observed in the Cs, Li-doped catalysts (Fig. 6). In

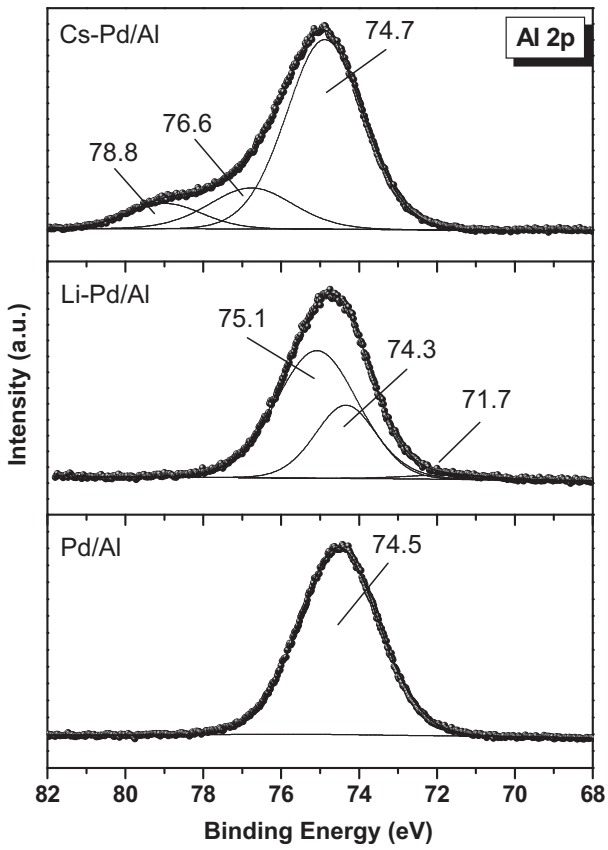

Fig. 4. XPS Al 2p spectra of un-doped Pd/Al, Li–Pd/Al and Cs-Pd/Al catalysts.

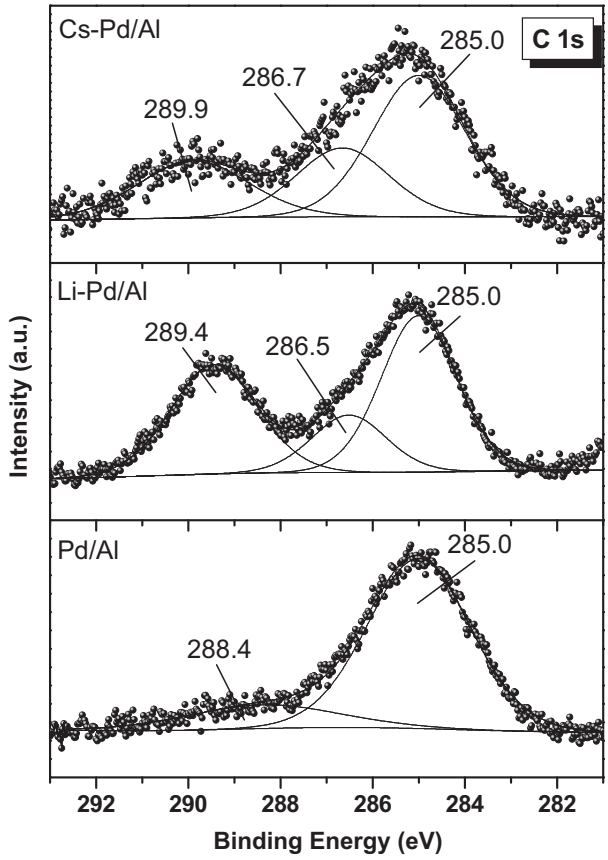

Fig. 5. XPS C 1s spectra of un-doped Pd/Al, Li–Pd/Al and Cs–Pd/Al catalysts.

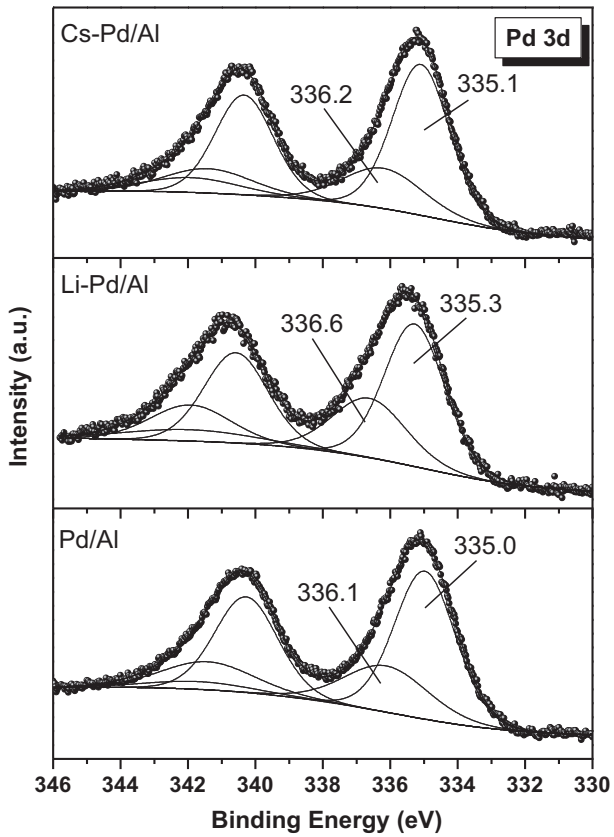

Fig. 6. XPS Pd 3d spectra of un-doped Pd/Al, Li–Pd/Al and Cs–Pd/Al catalysts.

the spectra of all three, un-doped and Li-, Cs-doped catalysts the Pd $3d_{5/2}$ peak component at binding energy of 335 eV characteristic of Pd-metal is the dominating [24]. The second palladium state observed in the spectra of all three catalysts is the one represented by small and highly energetic peak at ca. 336.1 eV. This energy is commonly ascribed to the $Pd^{\delta+}$ state which may be formed due to partial (surface) oxidation of Pd-metal particles.

Table 3 presents the microcalorimetric experiments of CO adsorption that provided data concerning the uptake of CO (μmol/g catalyst) by the catalyst samples, making it possible to determine the molar heats of adsorption of CO (kJ/mol CO). All the experiments used a comparable sample mass of ca. 0.16 g to fill the calorimetric cell, so that each sample contained ca. 30 μmol of Pd. Moreover, for all the catalysts studied, the adsorption of CO turned out to be totally irreversible at RT, as subsequent exposure of the samples to pure N_2 carrier yielded only a negligible desorption effect in each case.

Table 3 shows a relatively higher uptake of CO for two samples, K–Pd/Al and Cs–Pd/Al, respectively, 76.4 μmol/g and 81.1 μmol/g. For other samples the uptake ranges from 63.4 μmol/g to 66.3 μmol/g. This indicates that doping with the Li and Na cations does not change the CO sorption capability of such modified catalysts since the CO uptake of the respective samples is comparable to that of the parent, un-doped Pd/Al sample. The same is also true for the material doped with Cs in lower proportion, 0.5Cs–Pd/Al. In contrast, however, both the Cs-doped materials show remarkably higher molar heats of CO adsorption, 196 kJ/mol and 202 kJ/mol. This seems to suggest that no less than two different effects of Cs may be in operation in the so modified materials, separately responsible for increasing of the CO uptake, on one hand, and for increasing of the heat of adsorption, on the other. The higher molar heats of adsorption may indicate a stronger bonding of CO with palladium in the alkali doped catalysts, and especially strong in case of the most alkaline Cs promoter. This shows that the Cs may affect the electronic state of palladium stronger than the other alkaline modifiers can do. It also shows that the effect of increasing the molar heat is independent of the Cs/Pd ratio in the catalyst, suggesting that here the effect of promoter is somehow delocalized, i.e. the cesium is likely to change the electron density of Pd-particles using the alumina support as a mediator rather than by involving any kind of direct Pd–Cs interactions. Such direct interactions, on the other hand, seem more likely to be responsible for the effect of increasing of the uptake of CO, since it is more strongly dependent on the amount of the Cs promoter added. Hence, our results are in agreement with literature data presenting the interaction of alkali promoters with both, alumina support and Pd-particles [19,25,26].

Table 3
Microcalorimetric results of adsorption of CO.

Catalyst	CO uptake (μmol/g catalyst)	Molar heat of CO uptake (kJ/mol CO)
Pd/Al	64.9	155
Li–Pd/Al	66.3	176
Na–Pd/Al	63.9	157
K–Pd/Al	76.4	181
0.5Cs–Pd/Al	63.4	196
Cs–Pd/Al	81.1	202

3.1. Hydrogenation experiments

In typical analytical procedure commonly used in eAQ hydrogenation experiments, samples of the reaction mixture taken from the reactor were oxidized by air and extracted with water before chromatographic (GC, HPLC) analysis. The hydroquinone form (QH) is thermodynamically unstable and when contacted with air it is spontaneously and quickly oxidized forming hydrogen peroxide and restoring quinone (eAQ). Analogous reactivity is exhibited by tetra-form, although a longer time (ca. 15–30 min) is required for the quinone form to be restored completely. Thus, in the re-oxidized sample of reaction mixture used for chromatographic analysis the hydroquinone forms were absent and only the corresponding quinone forms were present. The OXO-isomer which is present in the reaction mixture (under hydrogen atmosphere) upon contacting with air isomerizes slowly to the hydroquinone form (QH) [10,11,27]. Our previous results showed that the isomerization of OXO to QH is relatively slow reaction and the concentration of OXO practically did not change during the time period of ca. 3 h from the moment of sample contacting with air [27]. Longer time of contacting with air resulted in slow decrease of OXO content whereas increased that of eAQ. This was associated with the isomerization of OXO to hydroquinone followed by its oxidation to the quinone form. Therefore, in order to determine the content of OXO (before it isomerizes to QH), all samples of reaction mixtures were analysed immediately after withdrawing from the reactor.

The literature data and our previous results revealed crucial role of OXO in the formation of degradation products [1,27]. The OXO isomer can be considered as the precursor for these products because the conversion of OXO by the hydrogenolysis reaction produces anthrone (eAN) which can be further transformed via aromatic ring hydrogenation to give other degradation products like (H_4eAN). Moreover, the hydrogenolysis reaction of eAN yields the next degradation products such as 2-ethylanthracene and its derivatives [1,8,9].

The hydrogen uptake curves obtained in the whole hydrogenation test performed at high concentration of catalysts (15 g/dm^3) are displayed in Fig. 7a, whereas the curves restricted to the initial stage of experiments are shown in Fig. 7b. In the initial stage of reaction featuring the reduction of eAQ to hydroquinone (quinone–hydroquinone stage) the rate of hydrogen uptake is very

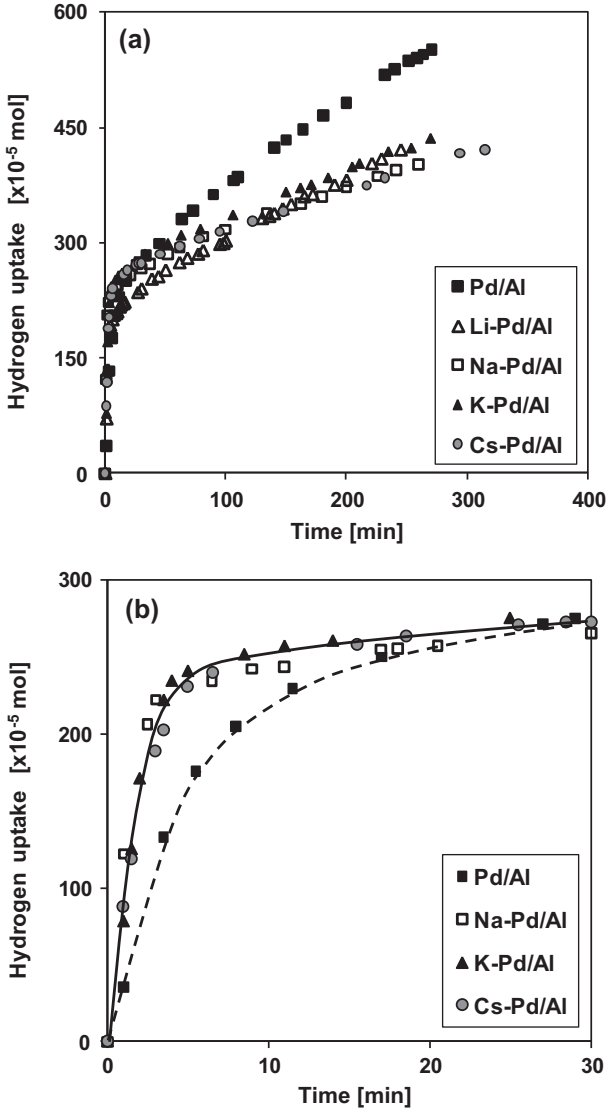

Fig. 7. Hydrogen uptake curves obtained in hydrogenation experiment performed at conditions: catalyst concentration 15 g/dm^3, eAQ concentration 20 g/dm^3.

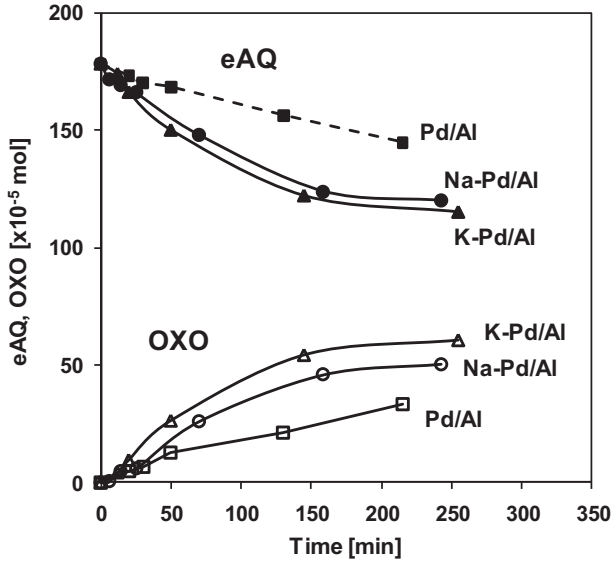

Fig. 8. The change of eAQ and OXO content in hydrogenation experiment performed at conditions: catalyst concentration 1 g/dm^3, eAQ concentration 20 g/dm^3.

high and after the consumption of ca. first equivalent of hydrogen a break on the hydrogen uptake curves appears thus evidencing almost complete hydrogenation of quinone to hydroquinone. Further hydrogenation occurs at a relatively low rate and is termed as "deep hydrogenation".

Two series of hydrogenation experiments were performed. In the series I experiments, the main reaction stage, e.g. hydrogenation of eAQ to hydroquinone was examined. The catalytic tests were carried out using very low catalysts concentration 1 g/dm^3. In the series II experiments, the hydrogenation tests were carried out at high concentration of catalysts (15 g/dm^3) and the course of "deep hydrogenation" stage was examined.

As shown in Fig. 7b on all alkali-doped catalysts the rate of hydrogen uptake in the first quinone–hydroquinone stage is higher compared to that on the un-doped Pd/Al catalyst. This may be considered to be the result of enhanced reactivity of alkali-doped catalysts for the C=O hydrogenation, similarly to what was observed in hydrogenation of various carbonyl compounds [15–17]. The presence of electropositive metal (Li, Na, K) was reported to facilitate the activation of the carbonyl C=O group via interaction of lone pair of C=O electrons with alkali modifiers.

The results obtained by XPS technique (Figs. 4–6) as well as CO chemisorption experiments (Table 3) reveal the interaction of alkali-promoters with alumina matrix. Moreover, the promoters affected to some extent the electronic state of palladium. These effects may lead to some changes in the adsorption ability of Pd-centres towards reagents, among them carbonyl groups, like C=O, C–OH. Therefore, it may be expected that enhanced reactivity towards quinone on alkali-doped catalysts would result in the formation of higher amount of H_2O_2. In order to verify this effect, the hydrogenation experiments were carried out under the same reaction conditions (catalyst concentration 1 g/dm^3) and the content of H_2O_2 formed after 50 min of reaction, i.e. the time corresponding to ca. 70% of quinone reduction was determined in oxidized solution (by titration method). The experiments were performed using un-doped Pd/Al and two cesium doped Cs–Pd/Al and 4Cs–Pd/Al catalysts. In the presence of all studied catalysts practically the same amount of H_2O_2 was determined, although the rate of hydrogen uptake was higher in the presence of alkali-doped catalysts. Thus, the observed effect may be associated with hydrogen spillover on the supports which is facilitated in the presence of alkali promoters. According to the literature observations among numerous variables affecting the effect of hydrogen spillover, electronic properties of the support exhibit an important role [28,29]. The effect of hydrogen spillover in the hydrogenation of eAQ seems to be interesting and further work is in progress in order to find a role of other experimental parameters.

However, in the quinone–hydroquinone stage, apart from the desired hydroquinone (QH) product, its isomer, OXO, the precursor of degradation products is formed. The nature of alkali promoter and its content (Me/Pd ratio) both affect the formation of OXO-isomer. From the very beginning of the first, quinone–hydroquinone stage, the content of eAQ continuously and slowly decreases whereas the content of OXO isomer grows. This effect is observed at both, low (Fig. 8) as well as at high (Fig. 9) catalyst concentrations. It can be observed that as the reaction progresses the content of OXO attains the maximum, which quite well correlates with a break on the hydrogen uptake curves. The decrease of eAQ content (number of moles) reflects quantitatively the increase of OXO content. The traces of H_4eAQ were observed only when the content of OXO reached the maximum i.e. when the rate of hydrogen uptake started to slow down. This implies that in "quinone–hydroquinone" stage all the reacted quinone was in the

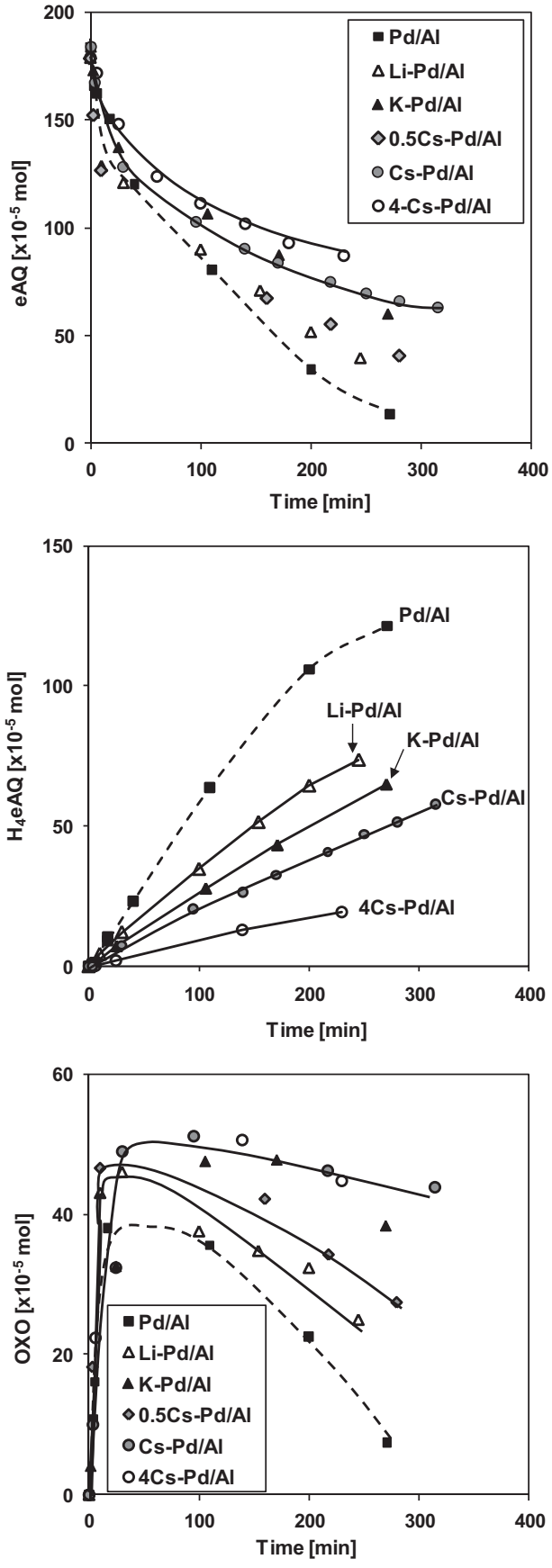

Fig. 9. Reagents distribution profile in "deep hydrogenation" experiments. Reaction conditions: catalyst concentration 15 g/dm^3, eAQ concentration 20 g/dm^3.

form of OXO-isomer and even if other products were formed their content was negligible.

As shown in Fig. 9 in the presence of alkali-doped catalysts the maximum content of OXO is higher than that formed on un-doped Pd/Al_2O_3 catalyst. Moreover, the maximum content of OXO depends on the nature, Cs, K, Na, of alkali-promoters (Figs. 8 and 9). The maximum content of OXO on K-doped catalyst is higher compared to that produced on Na-doped sample and both are higher compared to the content of OXO formed on un-doped Pd/Al catalyst (Fig. 8).

This effect cannot be explained on the basis of keto–enol tautomerization equilibrium for hydroquinone–OXO which was observed in the solution of these isomers (Scheme 1) [11–13]. In view of this scheme, under alkaline conditions the QH–OXO isomerization was shifted to the hydroquinone form, whereas acid conditions favoured the keto-form. An opposite effect is observed in the present work. It may be speculated that the tautomerization of hydroquinone molecules adsorbed on the centres of alkali-doped catalysts may be easier compared to the isomerization in solution, i.e. under conditions when the isomerization is accomplished due to the interactions with solvent and polarity of solvents is parameter determining its extent. However, it cannot be excluded that alkali promoters enhanced reactivity of catalysts towards the hydrogenation of quinone directly to the OXO isomer. This reactivity may be associated with facilitated effect of hydrogen spillover observed in the presence of alkali promoters. This effect is consistent with the recent results of Gao et al. [30] who stated by "in situ spectroscopic techniques" that on Pt/Al_2O_3 catalyst the hydrogenation of C=O group in acetophenone to C–OH was accomplished due to the presence of spilt-over hydrogen.

From the series II experiments the role of alkali promoters in the "deep hydrogenation" of eAQ can be clearly observed. The results reported by Petr et al. [8] as well as our previous studies [9] showed that in the course of "deep hydrogenation" stage the amount of H_4eAQH_2 formed was high whereas the amount of other products, i.e. eAN and in particular the products of the eAN hydrogenation (H_4eAN), was remarkably lower. Analogous effect can be observed from the present results.

The obtained reagent distribution profiles are displayed in Fig. 9. It can be seen that doping of catalyst with alkaline promoter results in strong inhibition of "deep hydrogenation" stage, i.e. the reactions transforming both reduced forms, hydroquinone QH and OXO. The nature and the content of alkali promoter in the catalyst are observed to determine the extent of reaction inhibition. This effect is evidenced by the data in Fig. 9 showing slow decrease of eAQ content vs. the time of hydrogenation experiment.

In the presence of all catalysts, un-doped Pd/Al_2O_3 and alkali doped samples the content of eAQ strongly decreases during the first few minutes of reaction whereas its further decrease is definitively slower. The initial strong decrease of eAQ content corresponds to the formation of OXO. As observed before (Fig. 8) the OXO isomer is formed during the first quinone–hydroquinone stage, reaching the maximum content at the breaking point on hydrogen consumption curve which corresponds to almost complete reduction of quinone (eAQ) form.

In this figure, the content of eAQ is given, because for the HPLC analysis re-oxidized solutions were subjected. However, as described before, the content of oxidized quinone form, eAQ, corresponds to that of hydroquinone (QH) form which occurred under hydrogen atmosphere. Therefore, the slow decrease of eAQ content in Fig. 9 may be considered as the decrease of hydroquinone (QH) content during the "deep hydrogenation" stage.

A complicated shape of eAQ decrease curves on all studied catalysts (Fig. 9) makes difficult the calculation of the conversion rates. Thus, in order to compare the activity of catalysts, the time required for 50% conversion during the "deep hydrogenation" stage

Table 4
"Deep hydrogenation" stage of eAQ.

Catalyst	Time[a] (min)	R (H_4eAQ) (mol min^{-1} g_{cat}^{-1})	R (eAN) (mol min^{-1} g_{cat}^{-1})	Selectivity at 50% eAQ conversion	
				S-Tetra (%)	S-eAN (%)
Pd/Al	76	1.29	0.29	44.6	8.9
Li–Pd/Al	100	0.78	0.30	39.2	16.8
0.5Na–Pd/Al	135	0.37		42.4	20
Na–Pd/Al	146	0.59	0.25	33.7	17.9
K–Pd/Al	143	0.54	0.18	38	13.6
0.5Cs–Pd/Al	86	0.59		26.9	14.6
Cs–Pd/Al	160	0.44	0.10	26	8.3
4Cs–Pd/Al	180	0.20	0.05	23.5	11.2

[a] Reaction time required for 50% eAQ conversion.

is assumed (Table 4). This time is the shortest for un-doped Pd/Al catalyst but it remarkably grows in the presence of all alkali-doped catalysts. This effect clearly demonstrates strong inhibition of QH conversion in "deep hydrogenation" stage in the presence of alkali-doped catalysts and the inhibition depends on the nature and the content of alkali promoter in the catalysts. At typical Me/Pd molar ratio of ~0.7, the smallest suppression is observed on Li-doped catalyst (Table 4). The inhibition is much more effective in the presence of Na, K and Cs-promoters and their content in catalyst plays a role. As the content of Cs-promoter increases, the activity of catalyst for the QH conversion decreases. The catalysts doped with various amounts of Na follow the same trend.

According to the literature data H_4eAQH_2 is formed via hydrogenation of phenyl ring in the hydroquinone QH and the reaction proceeds according to a dual site mechanism [4,5]. Therefore, the observed inhibition of QH conversion leads to decrease in the rate of H_4eAQH_2 formation and on all alkali-doped catalysts this rate is lower compared to that on Pd/Al catalyst (Table 4).

The higher alkalinity of the promoter going from Li to Cs, the rate of H_4eAQH_2 formation is lower (Table 4). Furthermore, when the content of Cs-promoter grows going from 0.5Cs–Pd/Al to 4Cs–Pd/Al catalysts, the rate of H_4eAQH_2 formation decreases even more. Thus, the ability of alkali-doped catalysts towards the hydrogenation of aromatic ring in the hydroquinone form is generally lower compared to that of the un-doped Pd/Al catalyst, and an extent of this effect appears to be determined by the nature of alkali-promoter.

The effect of alkali promoters in the subsequent transformation of OXO via hydrogenolysis reaction to anthrone product, eAN can be recognized from Fig. 10. Similarly to what observed in the series I experiments (Fig. 9), the maximum content of OXO isomer is higher on alkali-doped catalysts compared to the un-doped Pd/Al catalyst and the OXO content is especially high in the presence of Cs-doped catalysts. As the "deep hydrogenation" progresses the content of OXO decreases whereas the anthrone product, eAN, is formed. It should be noted, that no other products were observed by chromatographic analysis and the mass balance calculated for eAQ, OXO, H_4eAQ and eAN confirmed this observation.

However, the transformation of OXO to the anthrone product is slowed down as the result of alkali doping. Except from the Li-doped catalyst, on all other alkali modified catalysts, the rate of anthrone formation is lower compared to that on un-doped Pd/Al catalyst (Table 4). The nature of alkali promoter is of importance and the formation of anthrone is most effectively inhibited in the presence of Cs-doped catalysts. The inhibition effect of Cs-promoter is also a function of the Cs content as it clearly getting more pronounced going from 0.5Cs–Pd/Al to 4Cs/Pd–Al catalysts. Previous studies revealed that the transformation of OXO to anthrone is described by a first order reaction kinetics [4,5,27]. Hence, one can expect that the higher content of OXO on alkali-doped catalysts should result in higher rate of anthrone formation and consequently the content of anthrone should be higher. On the other hand, it is generally accepted that the hydrogenolysis reactions of C–OH to form C–H are catalysed by acid centres. Reducing of catalysts acidity by doping with alkali promoter (Na, K) resulted in strong suppression of C–OH hydrogenolysis during hydrogenation of acetophenone [18]. In the present work, as the alkalinity of the promoter increases going from Li to Cs, the formation of anthrone is more effectively suppressed. This may be ascribed to improved alkalinity of studied catalysts due to the alkali promoters.

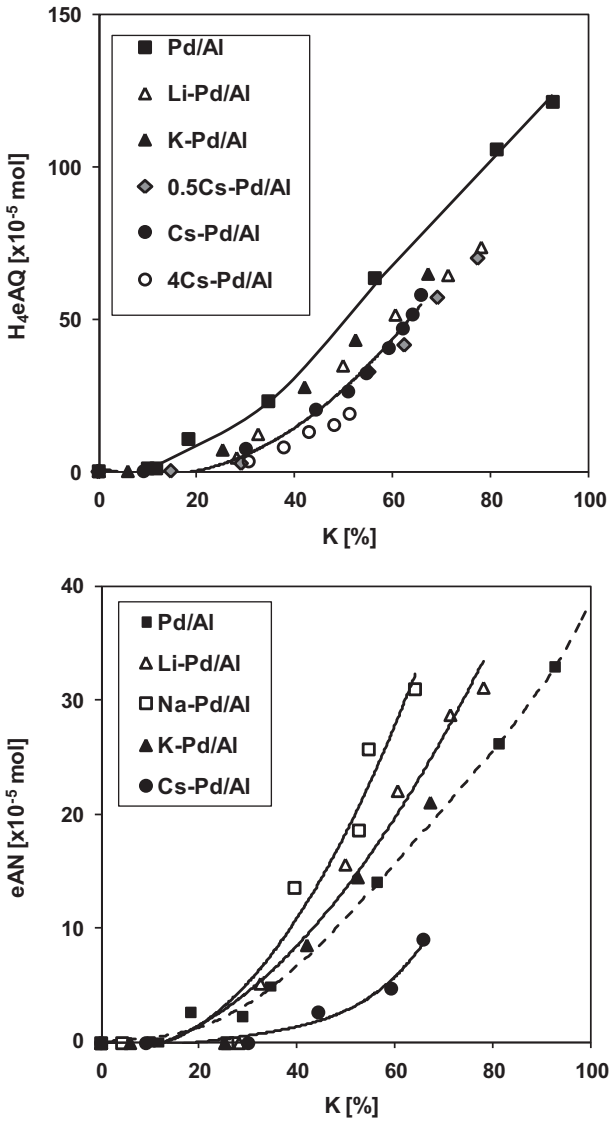

Fig. 10. The content of H_4eAQ and 2-ethylanthrone vs the conversion of eAQ. Reaction conditions: catalyst concentration 15 g/dm^3, eAQ concentration 20 g/dm^3.

This conclusion is supported by the observation that although on catalyst with more alkaline Cs promoter the content of OXO is the highest further conversion of OXO to anthrone is more effectively suppressed.

Let us compare the role of alkali promoter in the formation of H_4eAQH_2 and anthrone. The data in Table 4 show that relative to un-doped Pd/Al catalyst, in the presence of alkali-doped catalysts the formation of anthrone is less inhibited than the formation of H_4eAQH_2. This is evidenced by stronger decrease of the rate of H_4eAQH_2 formation than that of anthrone due to the presence of alkali promoters. As the result, on alkali-doped catalysts, the selectivity towards H_4eAQH_2 is lower than on Pd/Al catalyst. An opposite effect is observed relative to the selectivity to anthrone, which increases on alkali-doped catalysts. These selectivity results are supported by the relationships in Fig. 10 showing the content of H_4eAQH_2 and eAN moles against the conversion of eAQ, which was calculated according to Eq. (1). This conversion presents the whole amount of reacted eAQ, towards H_4eAQ, OXO and anthrone. At any given conversion of eAQ the content of H_4eAQ is the highest in the presence of un-doped Pd/Al catalyst and decreases on all alkali-doped catalysts. In particular, the low content of H_4eAQH_2 is formed in the presence of Cs-doped catalysts. For the entire range of eAQ conversions, the Li- and Na-doped catalysts both produced the content of anthrone considerably higher compared to that on the un-doped Pd/Al catalyst, whereas the K-doping has very little effect in this respect. In contrast, significantly lower content of anthrone is formed on Cs-doped catalyst (Fig. 10).

In summary, alkali promoters influenced reactivity of Pd/Al_2O_3 catalyst for the whole eAQ hydrogenation process. This reveals that acid–base properties of catalyst play an important role in hydrogenation of eAQ, similarly to what was observed in hydrogenation of number of carbonyl reactants. The effect of alkalinity has already been observed in our previous studies showing that high content of Na_2CO_3 in 0.5%Pd/SiO_2 catalyst enhanced the transformation of eAQ via hydrogenolytic reactions to form degradation products [4]. However, these studies did not provide data enabling evaluation the role of alkali-promoters in the course of particular reactions and especially in the formation and further transformation of OXO-isomer. Recently, the role of acid–base properties of Pd catalysts supported on SiO_2–Al_2O_3 with various content of SiO_2 in hydrogenation of eAQ was also studied by Feng et al. [31]. According to the authors, the acid sites on the surface of catalyst participated in the hydrogenation of eAQ because they acted as adsorption sites for eAQ molecules. The adsorbed eAQ molecules were subsequently activated and hydrogenated by spilt-over hydrogen species formed on metal surface. Similar effect involving the participation of acid–base sites of the supports for adsorption and activation of phenol molecules was postulated by other researches [19,21]. The acid–base properties of supports exhibited a primary role because they determined the geometry of phenol molecule adsorption whereas the reaction occurred between phenol chemisorbed on the support (phenolate species) nearby the metal particles and hydrogen chemisorbed on the Pd-sites [19]. In the presence of Pd catalysts supported on basic MgO, the phenol molecule was predominantly anchored to the surface through the oxygen atom forming phenolate form. On more acidic supports like alumina "coplanar" adsorption of phenol molecule involving O–H and aromatic ring was involved because of the interaction between benzene ring and the acid sites of the support. An analogous model was suggested for the hydrogenation of naphthalene [32]. The acidic sites of the support acted as adsorption sites for the aromatic compound, and in the vicinity of Pd particles these adsorbed species reacted with hydrogen spilt-over from the metal. The enhanced activity of Pd catalysts with high content of Na_2CO_3 for the formation of degradation product observed in our previous work [4] was also related to the facilitated adsorption of quinone in the carbonyl group-bonded configuration.

Thus, the enhanced alkalinity of the catalyst due to higher content of alkali promoter or more alkaline promoter facilitates the formation of OXO isomer whereas the reactions in "deep hydrogenation" stage are more and more inhibited. The Cs-doped catalysts exhibited the highest activity to OXO among all the catalysts tested and their activity in "deep hydrogenation" stage was most effectively inhibited. The molar heat of CO chemisorption was determined to be the highest for Cs-doped catalysts thus evidencing the strongest modification of catalyst properties by the Cs-species. This modification results in facilitated interaction of OXO with the catalyst and suppression of reactions in "deep hydrogenation" stage.

4. Conclusions

The presence of alkali (Li, Na, K, Cs) promoters plays an important role in the performance of Pd/Al_2O_3 catalysts for eAQ hydrogenation process. The XPS, EDS and TEM measurements show that alkali promoters are introduced into alumina matrix. The microcalorimertic experiments of CO adsorption prove the interaction of CO with catalysts leading to stronger bonding of carbon monoxide by alkali doped catalysts. The alkaline modifiers exhibit multiple effects on the whole eAQ hydrogenation process. The rate of the first quinone–hydroquinone stage increases whereas the rate of reactions in "deep hydrogenation" stage remarkably decreases. The nature of alkali promoter and its content (Me/Pd atomic ratio) in catalyst are of importance. As the alkalinity of promoter increases going from Li to Cs all the effects caused by their presence become stronger. Enhanced alkalinity of catalysts favours the formation of OXO, the isomer of hydroquinone. As the consequence, the content of OXO formed on alkali-doped catalysts is higher compared to that on un-doped Pd/Al_2O_3 sample. These effects are ascribed to stronger interactions between the catalyst and quinone reagents and may concern especially the OXO molecule. However, in the reagent adsorption the centres of support nearby the palladium particles may also participate by affecting the mode of reagents adsorption. The facilitated interaction of OXO with the catalyst results in the suppression of "deep hydrogenation" stage. On the other hand, the conversion of OXO to anthrone is strongly inhibited on alkali doped catalysts. This is ascribed to reduced acidity of catalysts due to alkaline promoters. Among all catalysts tested, the Cs-doped catalysts exhibit the highest activity for the formation of OXO whereas their ability to the formation of anthrone is strongly inhibited.

References

[1] Ulmann's Encyclopedia of Industrial Chemistry, vol. 13A, VCH, Weinheim, 1908, p. 443.
[2] W.M. Weigert, H. Delle, G. Kabish, Chem. Ztg. 99 (1975) 101.
[3] E. Santacesaria, M. Di Serio, A. Russo, U. Leone, R. Velotti, Chem. Eng. Sci. 54 (1999) 2799.
[4] E. Santacesaria, M. Di Serio, R. Velotti, U. Leone, J. Mol. Catal. 94 (1994) 37.
[5] E. Santacesaria, M. Di Serio, R. Velotti, U. Leone, J. Mol. Catal. 99 (1995) 151.
[6] Q. Chen, Chem. Eng. Process. 47 (2008) 787.
[7] R. Halder, A. Lawal, Catal. Today 125 (2007) 48.
[8] J. Petr, L. Kurz, Z. Bělohlav, L. Červený, Chem. Eng. Process. 43 (2004) 887.
[9] A. Drelinkiewicz, A. Waksmundzka-Gora, J. Mol. Catal. A 246 (2006) 167–175.
[10] S.W. Sjawcillo, W.I. Sawuszkina, E.M. Zhernowskaja, Zh. Obsh. Khim. 28 (1959) 1752.
[11] Houben-Weyl, Methoden der Organishen Chemie, Vol. 7, teil 3c, Georg Thieme Verlag, Stuttgart, 1979, p. 270.
[12] J. Houben, Das Antracen and die Antrachinone, Georg Thieme Verlag, Leizieg, 1929.
[13] K.H. Meyer, Annalen 379 (1911) 37.
[14] A. Drelinkiewicz, A. Waksmundzka-Góra, J. Mol. Catal. A 258 (2006) 1–9.
[15] P. Maki-Arvela, J. Hajek, T. Salmi, D.Yu. Murzin, Appl. Catal. A 292 (2005) 1–49.
[16] P. Gallezot, D. Richard, Catal. Rev. Sci. Eng. 40 (1998) 81–126.

[17] W. Koo-Amornpattana, J.M. Winterbottom, Catal. Today 66 (2001) 277–287, Pt/C.
[18] R.V. Malyala, C.V. Rode, M. Arai, S.G. Hedge, R.V. Chaudhari, Appl. Catal. A 193 (2000) 71–86.
[19] G. Neri, A.M. Visco, A. Donato, C. Milone, M. Malentacchi, G. Gubitosa, Appl. Catal. A 110 (1994) 49–59.
[20] U.R. Pillai, E. Sahle-Demessie, Appl. Catal. A 281 (2005) 31–38.
[21] S. Scire, C. Crisafulli, R. Maggiore, S. Minico, S. Galvagno, Appl. Surf. Sci. 93 (1996) 309–316.
[22] H.-B. Cho, J.-Ch. Lee, Y.-H. Park, Catal. Today 111 (2006) 417–422.
[23] M.M. Telkar, C.V. Rode, V.H. Rane, R.V. Chauhari, Catal. Commun. 6 (2005) 725–730.
[24] NIST Standard Reference Database 20, Version 3.2 (Web Version), National Institute of Standards and Technology, Gaithersburg, 2001.
[25] C. Qi, T. Bai, A. Lidun, React. Kinet. Catal. Lett. 54 (1995) 131–137.
[26] X.N. Mahata, K.V. Raghavan, V. Vishwanathan, Appl. Catal. A 182 (1999) 183–187.
[27] R. Kosydar, A. Drelinkiewicz, J.-P. Ghany, Catal. Lett. 139 (2010) 105–113.
[28] B.K. Hodnett, B. Delmon, Stud. Surf. Sci. Catal. 27 (1986) 53–78.
[29] R.T. Braunschweig, F. Roessner, J. Mol. Catal. A 127 (1997) 61–84.
[30] F. Gao, A.D. Allian, H. Zhang, S. Cheng, M. Garland, J. Catal. 241 (2006) 189–199.
[31] J.-T. Feng, H.-Y. Wang, D.G. Evans, X. Duan, D.-Q. Li, Appl. Catal. A 382 (2010) 240–245.
[32] J. Zheng, M. Guo, Ch. Song, Fuel Process. Technol. 89 (2008) 467–474.